CHARACTERISTICS OF FERROMAGNETIC FLUX FOCUSING LENS IN THE DEVELOPMENT OF SURFACE/SUBSURFACE FLAW DETECTOR

Buzz Wincheski, Jim Fulton, and Shridhar Nath
Analytical Services and Materials
107 Research Drive
Hampton, VA 23666

Min Namkung
NASA Langley Research Center
MS 231
Hampton, VA 23681

John Simpson
Lockheed Engineering and Sciences Co.
144 Research Drive
Hampton, VA 23666

INTRODUCTION

Electromagnetic NDE techniques have in the past steered away from the use of ferromagnetic materials. Although their high permeabilities lead to increased field levels, the properties of ferrous elements in the presence of alternating magnetic fields are difficult to determine. In addition, their use leads to losses which can be minimized through the use of low conductivity ferrites. In fact, the eddy current probes which do incorporate ferromagnetic materials have focused on these losses and the shielding which can be obtained by surrounding a probe with a high permeability, conducting material. Eddy current probes enclosed in conducting and magnetic shields have been used to prevent the generated fields from interacting with materials in the vicinity of the probe, such as when testing near material boundaries [1]. A recent invention has used ferromagnetic shielding to magnetically separate individual concentric eddy current probes in order to eliminate cross-talk between the probes so that simultaneous detection of different types of flaws at different depths can be achieved [2]. In contrast to the previous uses of ferromagnetic materials purely as magnetic shields, an electromagnetic flaw detector recently developed at NASA Langley Research Center takes advantage of the flux focusing properties of a ferromagnetic mild steel in order to produce a simple, effective device for the non-destructive evaluation of conducting materials [3].

The Flux Focusing Eddy Current Probe has been shown to accurately measure material thickness [4] and fatigue damage [5]. The straight forward flaw response of the probe

makes the device ideal for rapid inspection of large structures, and has lead to its incorporation in a computer controlled search routine to locate fatigue crack tips and monitor experimental fatigue crack growth experiments [5].

PROPERTIES OF FLUX FOCUSING LENS

The unique design feature of the flux focusing eddy current probe is the presence of a ferromagnetic material located between concentric drive and pickup coils. The drive coil is wound around the cylindrical lens and a high turn pickup coil is placed in the interior of the ferromagnetic cylinder. The change in the field distribution caused by the presence of the flux focusing lens shields the pickup coil from the direct mutual interaction with the drive coil and produces a high field concentration at the outer edge of the pickup coil.

In the absence of the ferromagnetic lens the magnetic field distribution in the area of the pickup coil would be that in the interior of an air core solenoid. An exact solution for this problem is available in the literature [6]. The magnetic field components of a single turn coil in air are given in cylindrical coordinates by:

$$B_r = \left(\frac{J}{c}\frac{2z}{r\sqrt{[\,(a+r)^2+z^2]}}\right)\left[-K+\frac{a^2+r^2+z^2}{(a-r)^2+z^2}E\right], \qquad (1)$$

$$B_z = \left(\frac{J}{c}\frac{2}{\sqrt{[\,(a+r)^2+z^2]}}\right)\left[K+\frac{a^2-r^2-z^2}{(a-r)^2+z^2}E\right], \text{ and} \qquad (2)$$

$$B_\varphi = 0, \qquad (3)$$

where r = radial distance to the center of the coil, z = axial distance from the center of the coil, J = current in the wire, c = speed of light, a = radius of the coil, and K and E are complete elliptic integrals of the first and second kind.

$$K = \int_0^{\frac{1}{2}\pi} \frac{d\theta}{\sqrt{(1-k^2\sin^2\theta)}},\ E = \int_0^{\frac{1}{2}\pi} d\theta\sqrt{(1-k^2\sin^2\theta)}\,, \qquad (4)$$

with

$$k^2 = \frac{4ar}{[\,(a+r\,)^2+z^2)\,]}. \qquad (5).$$

The field inside an N turn solenoid would then be the sum of the contribution from each turn of the coil:

$$\bar{B} = \sum_N (B_r\hat{r} + B_z\hat{z}) \qquad (6).$$

The flux given in (6) is displayed in a vector plot for a unit length solenoid with a=l/2 in Fig. 1. The fields inside the solenoid are fairly uniform throughout the length of the coil, with only a slight bending occurring as the flux enters and exits from the interior of the coil. The magnetic flux permeates the entire interior region of the coil, with the highest normal field levels occurring along the centerline.

The field distribution inside the Flux Focusing Probe was not analytically determined because the presence of the ferromagnetic lens dramatically increases the complexity of the

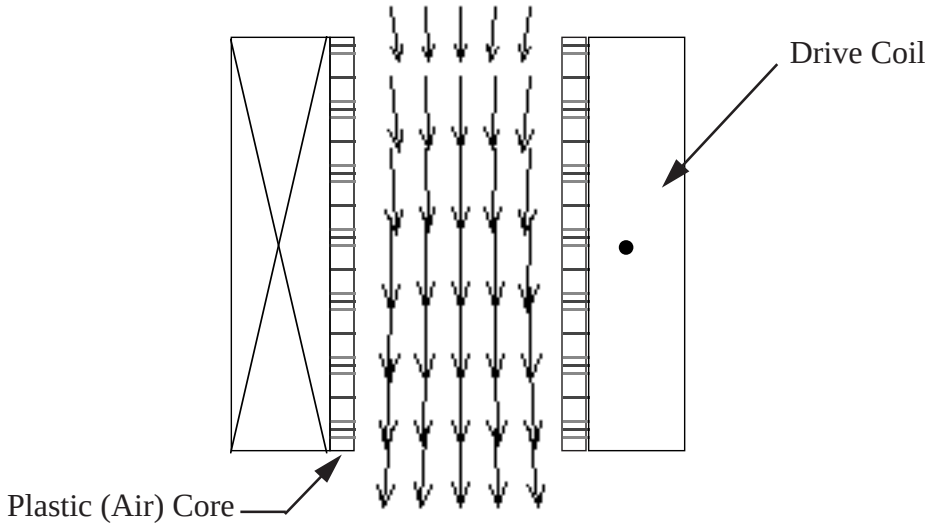

Fig. 1. Calculated field flow through an air-core solenoid.

problem. Experimental and finite element methods were instead used to map the magnetic field flow through the probe.

Experimental determination of the field flow in the interior of the probe was accomplished using miniature pickup coils to scan the area inside the ferromagnetic lens. The normal and radial field components were separately measured using pickup coils wound with their axes parallel and perpendicular to the normal axis of the flux focusing probe, respectively. A lock-in amplifier referenced to the drive signal of the primary coil was used to monitor the induced voltage across the miniature pickup coils, recording both the amplitude and phase at each measurement location. The instantaneous amplitude at each point was then calculated for both field components as the RMS amplitude multiplied by the sine of the phase, $A=R*\sin\varphi$.

HIGH FREQUENCY CHARACTERIZATION

Fig. 2 displays a vector plot of the experimentally determined field flow inside the Flux Focusing Eddy Current Probe operating at 100 kHz. A schematic illustration of the field flow throughout the space surrounding the probe is also given in the figure. The presence of the ferromagnetic sleeve dramatically alters the uniform field flow seen in Fig. 1 for an air-core solenoid. The magnetic flux, seeking the path of least reluctivity, rapidly flows into the flux focusing lens. The field lines which reach the interior of the probe have curled around the ends of the ferromagnetic cylinder on a wide loop around the primary windings, as illustrated in Fig. 2b. When the probe is placed above a conductor these field lines are attenuated by the skin depth effect [7] as they diffuse into the test sample. The long path length of the fields around the ferrous lens results in a total shielding of the interior of the probe from the primary fields, resulting in a null signal, at high frequencies.

An axisymmetric finite element model of the flux focusing probe was constructed in order to further characterize the field distribution of the device. The results, pictured in Fig 3, confirm the experimental results for the field flow inside the probe. The vector plot of the magnetic field also shows a high field concentration directly under the flux focusing lens wall. These field lines produce a high density eddy current ring at the outer edge of the pickup coil when a conducting material is inspected. These eddy currents are responsible for

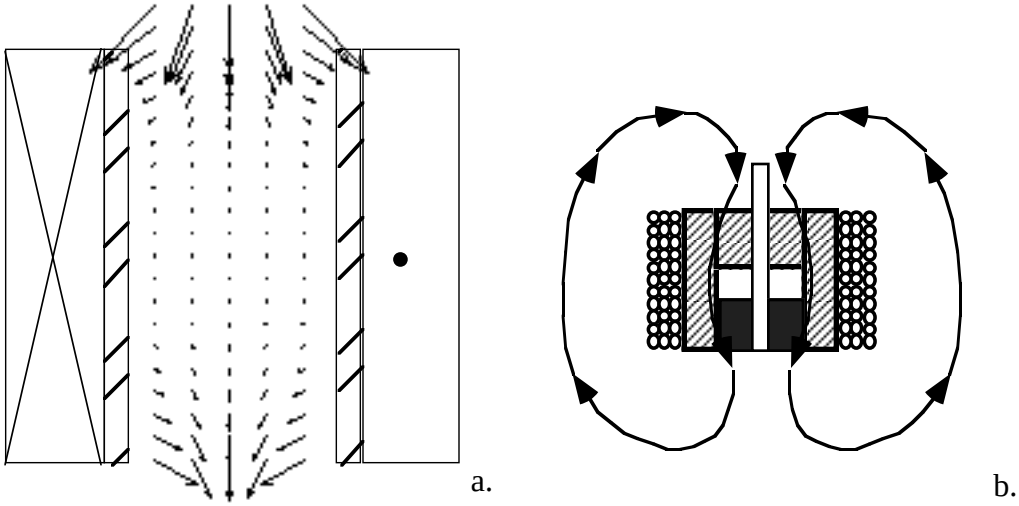

Fig. 2. Experimentally determined field flow through Flux Focusing Probe at operating frequency of 100 kHz (a), and schematic representation of closed loop of field path around primary windings (b).

the fatigue crack detection properties of the probe [5,8].

LOW FREQUENCY CHARACTERIZATION

The detection of subsurface flaws requires that the operating frequency of an eddy current device be lowered to a value such that the skin depth is comparable to the depth at which the part is to be inspected [9].

$$f \cong \frac{1}{(\pi\mu\sigma)\ (depth\,(m))^2} \qquad (7)$$

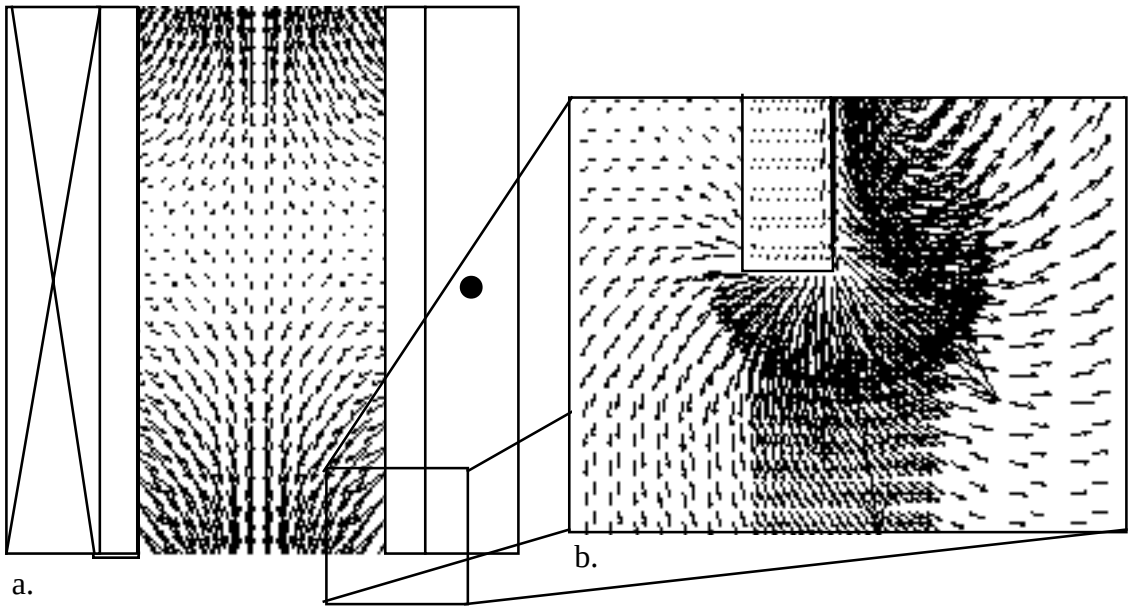

Fig. 3. Finite element results for magnetic field flow inside (a) and at end of flux focusing lens (b). Results confirm experimental findings displayed in Fig. 2, and show high field concentration directly under cylindrical lens.

The detection of corrosion damage at the back surface of a 1mm thick aluminum alloy plate with permeability $\mu_{al} = 4\pi * 10^{-7}$ H/m and conductivity $\sigma_{al} = 1.7 * 10^{7}$ mho/m, for example, would suggest an operating frequency of approximately 15 kHz. The ideal testing frequency could vary significantly from this initial calculation due to the simplifying assumptions made in obtaining the skin depth equation [7]. A swept frequency measurement centered around the value as calculated above is often used in order to guarantee a thorough inspection of the part.

Low frequency characterization of the flux focusing lens was performed through experimental and finite element methods similar to those used in characterizing the high frequency operation. The magnetic field flow through the interior of the probe was experimentally measured at an operating frequency of 10 kHz in order to determine the effect of the ferrous lens on the magnetic field at low frequencies. A vector plot of the fields in the interior of the probe is displayed in Fig. 4. The results are similar to those displayed in Fig. 2, with the interior magnetic field curling around the ends of the lens before heading into the ferrous material. The behavior of the fields in the center of the probe, however, is markedly different from that obtained at 100 kHz. Fig. 4b. shows the magnitude of the normal magnetic field increasing in the center of the coil while the direction has reversed from a downward to an upward traveling field.

The cause of the field reversal in Fig. 4 was found to be due to the penetration of the primary magnetic field through the lens wall and into the interior of the probe. As the primary field diffuses into the lens wall it will undergo an exponential decay in amplitude as given by the skin depth equation [7]

$$B = B_0 exp\,(-x\sqrt{\pi f \mu \sigma}) \qquad (8).$$

At low frequencies the attenuation constant is not large enough to completely shield the interior of the probe from the fields diffusing through the wall. The maximum effect of these fields will be at the midpoint of the drive coil length, decreasing as the ends of the drive coil are approached. Fig. 5 displays finite element results for the eddy current density in the flux

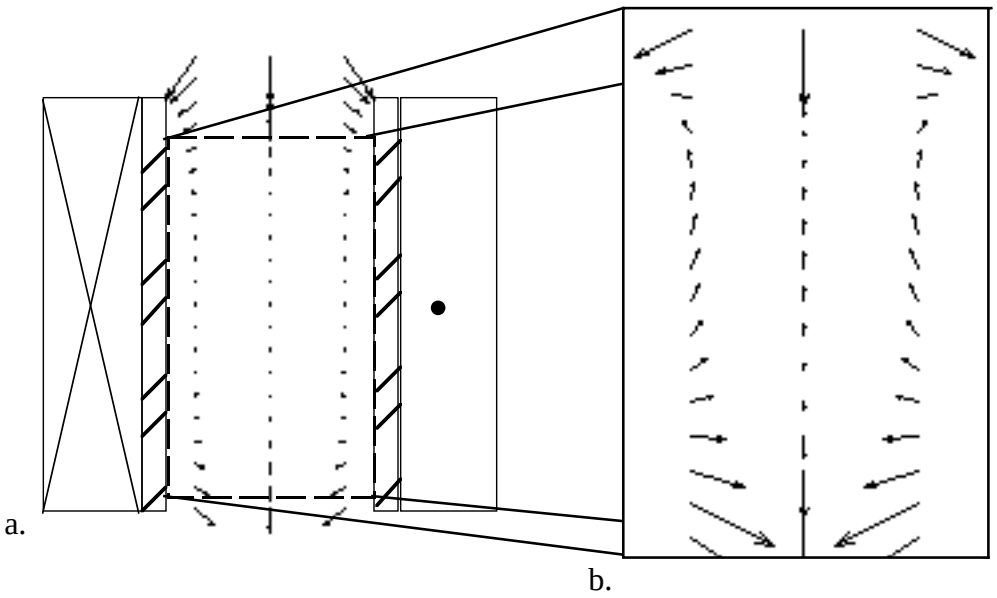

Fig. 4. Experimental results for magnetic field flow through the interior of the Flux Focusing Probe at an operating frequency of 10 kHz. The fields in the center of the probe are seen to begin to increase in magnitude and reverse direction.

focusing lens at a 10 kHz drive. The eddy current density is seen to extend completely through the lens wall at the center of the probe, decreasing in magnitude as the ends of the probe are approached. At the ends of the probe the effect of the field curling around the lens can be seen, producing an increase in the eddy current density where the field enters the lens. The eddy currents produced by the two effects, diffusing through the wall and curling around the lens, converge at a point roughly one fourth of the shield length away from the ends of the probe. This distance corresponds with the point of field reversal in the interior of the probe shown in Fig. 4.

The field inside the probe is then a combination of the fields diffusing through the lens wall and curling around the ends of the wall. The effect of the fields curling around the lens is greatest where the effect of the fields diffusing through the lens is smallest, at the ends of the probe. Likewise, in the center of the probe, the fields diffusing through the wall will be at their maximum level when the fields passing around the end of the lens are at their minimum level.

As the magnetic field diffuses through the lens wall a linear phase shifting of the field will occur according to [7]:

$$\varphi = \varphi_0 x\sqrt{\pi f \mu \sigma} \qquad (9).$$

The change in phase between the fields curling around the lens, at the top and bottom of the probe, and the fields diffusing through the lens, at the center of the probe, was measured across a frequency range of 5 - 17.5 kHz. Experimental data was acquired using miniature field sensors positioned at the interior of the phase wall. Fig. 6 displays the phase difference between the magnetic field at the top of the probe, resulting from fields curling around the lens wall, and the field at the center of the probe, resulting from fields diffusing through the lens wall. The near linear increase in phase delay with the square root of the frequency displayed in the figure is predicted from (9). The phase delay of the magnetic field propagating completely through the lens wall is approximately 180° for a 10 kHz drive. This phase shifting of the magnetic field causes the reversal in direction of the field in the interior of the lens seen in Fig. 4.

The magnitude of the field diffusing through the lens wall is attenuated as $exp\,(-\sqrt{f})$ (8) so that the increasing phase delay seen in Fig. 6 is accompanied by a rapid decrease in field level at the center of the probe. The amplitude of the field diffusing through the lens

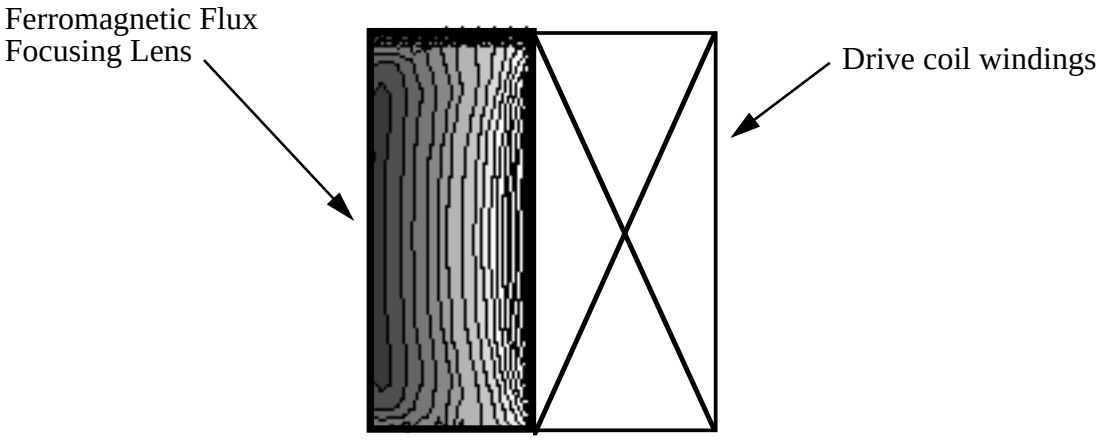

Fig. 5. Eddy current density in flux focusing lens wall at 10 kHz drive.

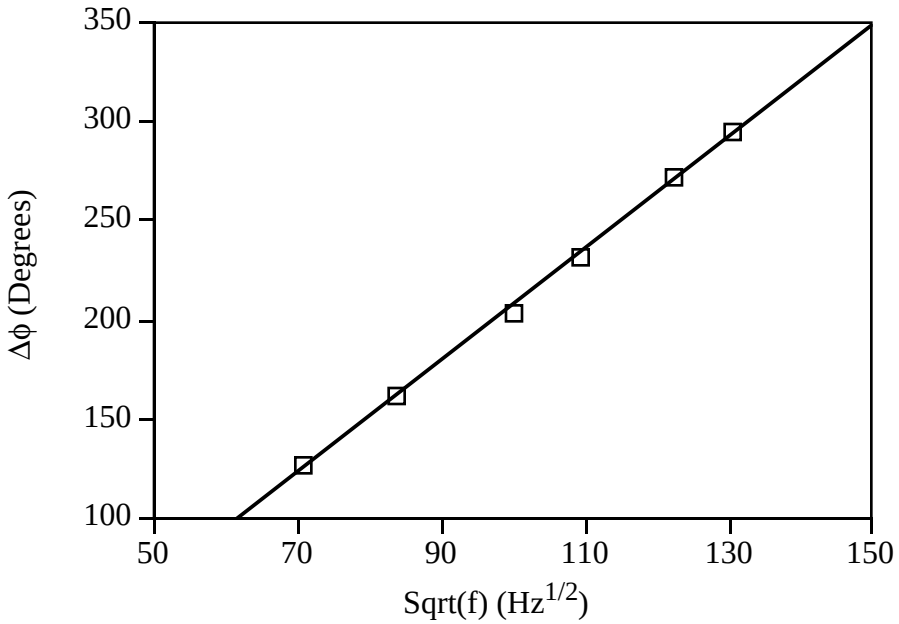

Fig. 6. Plot of the phase delay of the magnetic field diffusing through the flux focusing lens as a function of the square root of the frequency.

was seen to approach background levels at approximately 20 kHz.

Material loss measurements often must be made at frequencies where a large component of the fields in the interior of the probe are due to the magnetic field diffusing through the lens wall. Material thickness measurements rely on sensing changes in the magnetic field curling around the lens wall as it diffused through the material under test [3]. These fields make a wide loop around the primary windings, penetrating deep into the material under test. Maximum sensitivity to material thickness changes will occur when the effect of the fields curling around the lens dominates the field diffusing through the lens at the location of the field sensor. This can be accomplished by placing the pickup coil close to the bottom of the probe, not extending above approximately 1/4 the length of the lens. In this area the main field components have been shown to be due to fields curling around the bottom of the lens.

SUMMARY

In this paper a new electromagnetic flaw detector developed at NASA Langley Research Center has been introduced. The device takes advantage of the flux focusing properties of a ferromagnetic mild steel in order to produce a simple, effective tool for the accurate measurement of material thickness and detection of fatigue cracks. The properties of the flux focusing lens have been explored through experimental and numerical methods.

In characterizing the lens, concentration has been focused on determining the spatial variations in the magnetic field as well as the direction of field flow throughout the space surrounding the probe. The properties of the device have been studied over a frequency range of 5-100 kHz, and results explained in terms of classical electromagnetic relationships.

REFERENCES

1. *Nondestructive Testing Handbook, Volume Four*, edited by Paul McIntire (American Society for Nondestructive Testing, Inc., 1986).
2. William G. Clark, Jr., and Michael J. Metala, "Multiple Coil Eddy Current Probe and Method of Flaw Detection," U.S. Patent Number 4,855,677 (1989).
3. John W. Simpson, B. Wincheski, M. Namkung, J.P. Fulton, R.G. Todhunter and C.G. Clendenin, "Flux-Focusing Eddy Current Probe and Method for Flaw Detection," Patent Pending.
4. B. Wincheski, M. Namkung, J.P. Fulton, and S. Nath, Presented at 1993 *Review of Progress in QNDE,* Brunswick, ME (August 1-6, 1993).
5. M. Namkung, C.G. Clendenin, J.P. Fulton, and B. Wincheski, Presented at 1993 *Review of Progress in QNDE,* Brunswick, ME (August 1-6, 1993).
6. L.D. Landau, E.M. Lifshitz and L.P. Pitaevskii, *Electrodynamics of Continuous Media,* (Pergamon Press, New York, 1984).
7. H.L. Libby, *Introduction to Electromagnetic Nondestructive Test Methods,* (John Wiley & Sons, Inc., New York, 1971).
8. B. Wincheski, J.P. Fulton, S. Nath, N. Namkung, and J.W. Simpson, "Self-Nulling Eddy Current Probe for Surface and Subsurface Flaw Detection", Submitted to *Materials Evaluation.*
9. D.J. Hagemaier, "Eddy Current Impedance Plane Analysis," Presented to *1982 Air Transport Association Non-Destructive Testing Forum,* Atlanta, GA (September 14-16, 1982).